

Adaptive Computer-Aided Tuning of Coupled-Resonator Diplexers With Wire T -Junction

Ping Zhao, *Student Member, IEEE*, and Ke-Li Wu, *Fellow, IEEE*

Abstract—This paper is devoted to theoretical and practical issues concerning computer-aided tuning (CAT) of coupled-resonator diplexers with tapped wire T -junction. Special attentions are paid to the following aspects: 1) finding an appropriate circuit model to represent the tapped wire T -junction; 2) developing a legitimate transformation strategy to obtain the coupling matrix of the right form corresponding to the topology of the diplexer containing a tapped wire T -junction; and 3) proposing an adaptive CAT scheme that takes stray couplings into account in a dynamically optimized target coupling matrix. A conventional combline diplexer and a helical resonator diplexer are used as examples to demonstrate the circuit model extraction procedure and the adaptive CAT concept, showing the effectiveness and robustness of the proposed adaptive CAT method for practical applications.

Index Terms—Computer-aided tuning (CAT), coupling matrix, cross coupling, microwave diplexer, nonresonant node (NRN), rational approximation.

I. INTRODUCTION

WITH the proliferation of mobile communication systems, microwave diplexers are needed in unprecedented large quantities. To manufacturers, a major concern is how to timely and cost-effectively manufacture the diplexers in a large quantity. To this end, developing a robotic automatic tuning system which can ensure a high yield in tuning a large batch of same diplexer products becomes a high priority.

In the past years, various approaches for computer-aided tuning (CAT) of bandpass filters have been extensively investigated [1]–[8]. Among all the methods, rational fitting of characteristic functions from the measured or simulated frequency-domain responses using Cauchy method [5]–[7] or vector fitting (VF) [8] has been proven to be an effective way to extract the system poles and zeros, from which the coupling matrix corresponding to coupling topology can be constructed.

CAT for diplexers was first explored by applying Cauchy method to a diplexer circuit model [9] without considering practical issues such as parasitic couplings and measurement

noise. Another attempt to CAT for diplexers is by first deducing the responses of two channel filters from S -parameters of the diplexer and the junction [10], and then diagnosing each filter individually. This approach requires that the accurate junction model is available and the ports connecting the junction and channel filters are well-defined, which are usually impermissible in practical applications.

Recently the model-based vector fitting (MVF) method is proposed for recovering the characteristic functions from noise-contaminated measured responses of a diplexer. However, the procedure for circuit model extraction in [11] only deals with diplexers with a common resonator. The transformation strategy lacks of generality for other forms of practical diplexers and stray couplings that inevitably exist in practical applications are not addressed.

In practice, two types of junctions are widely used in diplexers in wireless communication industry: the common resonator junction and the tapped wire T -junction. The tapped wire T -junction requires smaller I/O coupling associated with the common port. Besides, a tapped wire T -junction is more compact in size. In terrestrial communication systems, tapped wire T -junction diplexers that are composed of two high-order channel filters with multiple transmission zeros (TZs) are commonly seen to achieve high level of isolation between closely spaced Tx and Rx channels.

This paper is devoted to both theoretical and practical issues related to CAT of coupled-resonator diplexers with tapped wire T -junction. Specifically, the contributions are made as follows.

- 1) A proper circuit model for a tapped wire T -junction suitable for CAT process of a diplexer.
- 2) A canonical form of diplexer and a general transformation strategy to obtain the coupling matrices of two channel filters that are joined by a tapped wire T -junction.
- 3) An adaptive CAT strategy that can effectively deal with stray couplings for enhancing tuning yield in mass production.

This paper is organized in the following way. In Section II, a proper circuit model for the tapped wire T -junction is found, which allows the utilization of MVF method to extract the Y -parameter rational functions to obtain a three-port transversal coupling matrix in Section III. In Section IV, a new general coupling matrix transformation strategy is introduced to transform the transversal matrix to the right form corresponding to the topology of diplexer hardware, with which one-to-one correspondence between the matrix entries and physical tuning elements is established. In Section V, the concept of adaptive CAT is introduced, followed by conclusions.

Manuscript received December 22, 2016; revised March 14, 2017; accepted March 18, 2017. Date of publication April 12, 2017; date of current version October 4, 2017. This work was supported in part by the Postgraduate scholarship of The Chinese University of Hong Kong and in part by the Development and Reform Commission of Shenzhen Municipality under Grant Shen Fa Gai (2013) 1673.

The authors are with the Department of Electronic Engineering, The Chinese University of Hong Kong, Hong Kong (e-mail: pzha@ee.cuhk.edu.hk; kllwu@ee.cuhk.edu.hk).

Color versions of one or more of the figures in this paper are available online at <http://ieeexplore.ieee.org>.

Digital Object Identifier 10.1109/TMTT.2017.2686852

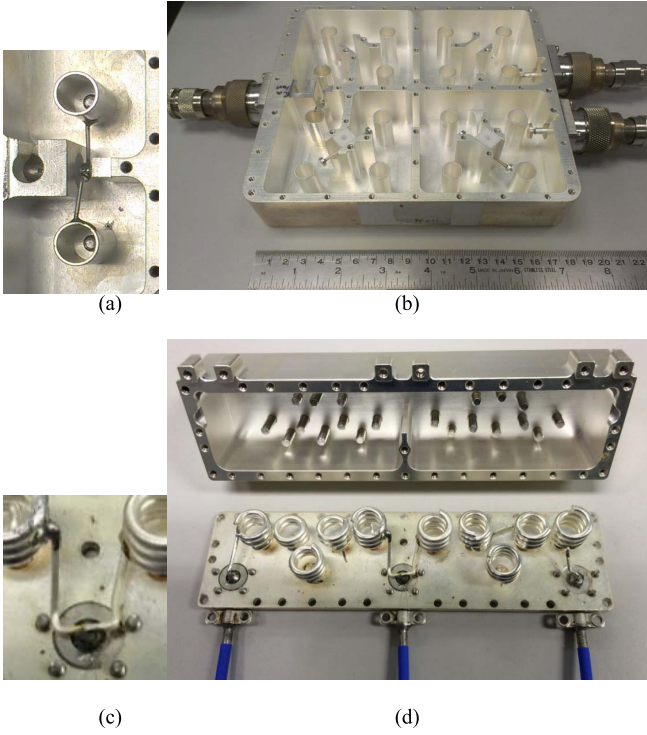


Fig. 1. Photographs of diplexers with tapped wire T -junctions. (a) Tapped wire T -junction in a combline diplexer. (b) Combline diplexer. (c) Wire T -junction in a helical resonator diplexer. (d) Helical resonator diplexer.

II. CIRCUIT MODEL FOR TAPPED WIRE T-JUNCTION

Tapped wire T -junction is a simple but widely used structure to compactly combine two channel filters. For example, Fig. 1(a) and (c) shows wire T -junctions in a coaxial combline diplexer and a helical resonator diplexer, respectively.

A tapped wire T -junction can be modeled by a nonresonant-node (NRN) junction, as shown in Fig. 2(a), provided that: 1) the lengths of the tapped wires are in small fractions of the wavelength and 2) the bandwidth of the device is narrow to moderate. Alternatively, the junction can also be modeled by a Δ -model, as shown in Fig. 2(b). By the Δ -to- Y transformation [12] and the phased-inverter to frequency-invariant reactance (FIR)-inverter transformation [13], the two circuits are equivalent to each other with a constant phase length θ at the common port of the NRN circuit model.

In this paper, the Δ -circuit model is adopted in the CAT program for two reasons: 1) it does not contain an NRN, so the whole network can be obtained by similarity transformations from the transversal coupling matrix and 2) the Δ -circuit junction model is convenient for extraction of phase loading at the common port.

To clarify the second point, in both junction models, as s approaches $j\infty$, the capacitors will become short-circuited. Hence, for the NRN model in Fig. 2(a)

$$Y_{in_1}|_{s \rightarrow j\infty} = 0 \quad Y_{in_2}|_{s \rightarrow j\infty} = 0. \quad (1)$$

Consequently, the input admittance seen from the common port is

$$Y_{in}|_{s \rightarrow j\infty} = \frac{M_{01}^2}{jb_1 + Y_{in_1} + Y_{in_2}}|_{s \rightarrow j\infty} = \frac{M_{01}^2}{jb_1} \quad (2)$$

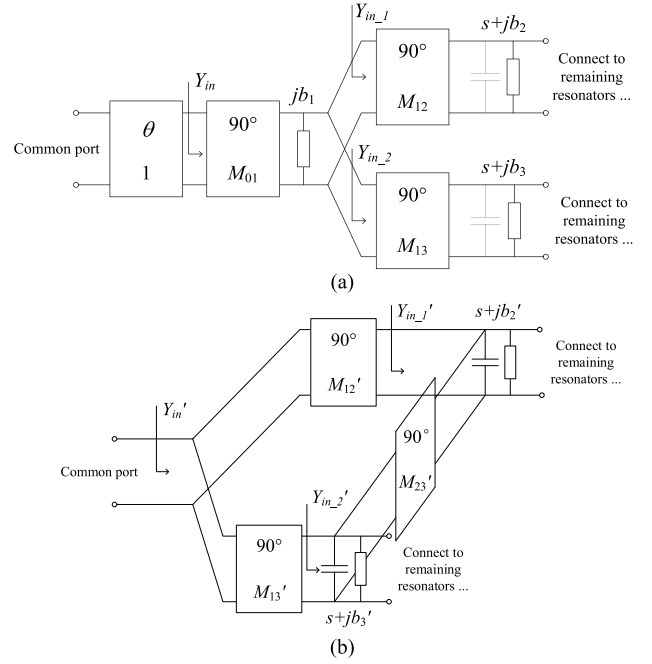


Fig. 2. Proposed circuit models for tapped wire T -junction. (a) NRN Y -circuit model with a constant phase length at the common port. (b) Δ -circuit model.

and the reflection coefficient at the common port is

$$\Gamma|_{s \rightarrow j\infty} = \frac{1 - Y_{in}}{1 + Y_{in}}|_{s \rightarrow j\infty} = \frac{1 + jM_{01}^2/b_1}{1 - jM_{01}^2/b_1} \quad (3)$$

whose phase tends to be a nonzero constant

$$\arg(\Gamma)|_{s \rightarrow j\infty} = 2 \tan^{-1} \frac{M_{01}^2}{b_1}. \quad (4)$$

This constant is unknown prior to the determination of M_{01} and b_1 . As a result, it is not easy to de-embed the phase loading and the transmission line at the common port with the NRN Y -circuit model. On the other hand, for the Δ -circuit model in Fig. 2(b)

$$Y'_{in_1}|_{s \rightarrow j\infty} = \infty \quad Y'_{in_2}|_{s \rightarrow j\infty} = \infty. \quad (5)$$

As a result, the input admittance becomes

$$Y'_{in}|_{s \rightarrow j\infty} = 0 \quad (6)$$

and the reflection coefficient at the common port are found to be

$$\Gamma'|_{s \rightarrow j\infty} = 1 \quad \arg(\Gamma')|_{s \rightarrow j\infty} = 0. \quad (7)$$

With the Δ -circuit junction model adopted, the phase of the reflection coefficient at the common port asymptotically tends to zero.

III. MODEL EXTRACTION

With the Δ -circuit model for the wire T -junction, the transmission line and phase loading at the common port can be removed together by the method introduced in [4]. Then the MVF technique [11] can be used to extract system poles and zeros of Y -parameters to construct a three-port transversal coupling matrix.

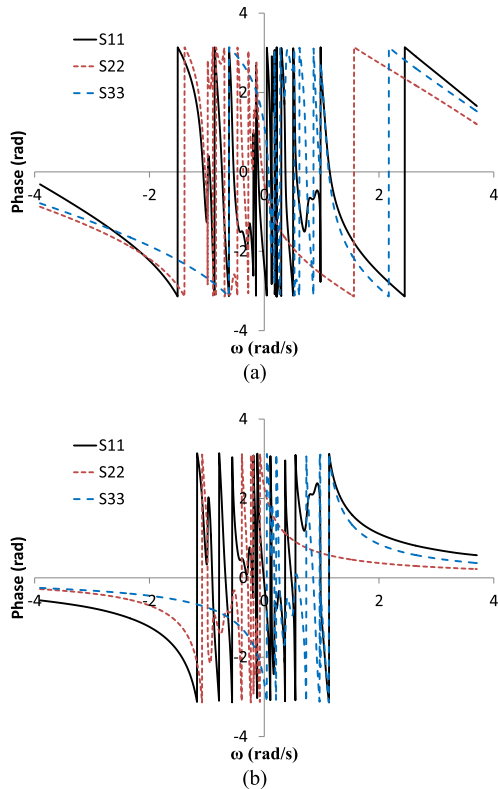


Fig. 3. (a) Phases of the raw measured reflection coefficients at three ports. Asymptotic lines can be observed due to the phase loading and transmission line effect. (b) Phases of the reflection coefficients after the deembedding of phase loading and transmission line effect at three ports.

A. Combline Diplexer

The first example is a combline diplexer as shown in Fig. 1(b). The diplexer body takes a volume of 185 mm × 165 mm × 35 mm. The lengths of the wires connecting the junction to the first two resonators of the upper and lower band filters are 20.1 and 14.7 mm, respectively. The height of the tapping points on the inner rods are about 24 and 10 mm, respectively. The cavity size of a single resonator is 38 mm × 35 mm × 30 mm, and the height of the inner rod is 25 mm.

The lower and upper frequency bands of the combline diplexer are 1.691–1.789 GHz and 1.821–1.929 GHz, respectively. The measured responses are transformed to the lowpass domain by

$$s = j\omega = j \frac{f_0}{\text{BW}} \left(\frac{f}{f_0} - \frac{f_0}{f} \right) \quad (8)$$

where $f_0 = 1.806$ GHz, and $\text{BW} = 0.238$ GHz.

With the Δ -junction model, the transmission line and phase loading at the common port can be removed as an ordinary port. Fig. 3(a) and (b) shows the phases of the reflection coefficients of one tuning state before and after the deembedding process, respectively.

The routing diagram of the combline diplexer with the Δ -junction model is depicted in Fig. 4. By the minimum path rule [14], the number of TZs can be determined for each transfer function. The shortest path between ports 1 and 2 is P1-8-7-5-4-1-P2, which passes through five resonators. There are totally 16 resonators. Theoretically, there

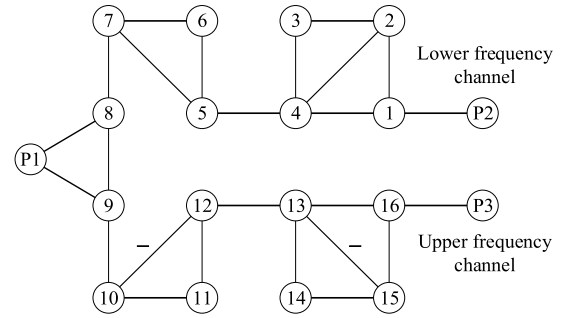


Fig. 4. Routing diagram of the combline diplexer. Hollow circles marked P1–P3 represent three ports. Hollow circles with numbers inside represent resonators. Straight lines are either interresonator couplings or I/O couplings.

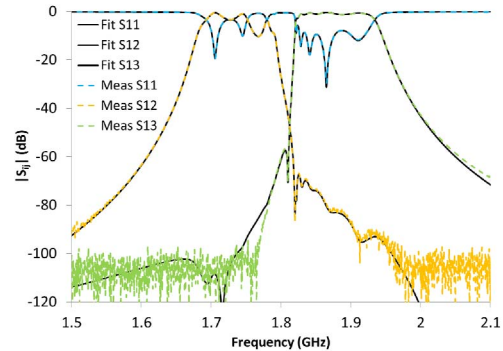


Fig. 5. Measured data and calculated responses of the extracted transversal coupling matrix of the combline diplexer.

are $16 - 5 = 11$ TZs in S_{12} (Y_{12}). By the same token, it can be told that there are 11 TZs in S_{13} (Y_{13}) and 6 TZs in S_{23} (Y_{23}). To take possible parasitic couplings into account, a practical estimation of the numbers of TZs for S_{12} , S_{13} , and S_{23} are 12, 12, and 8, respectively. With the estimated numbers of TZs, one can set appropriate orders of numerators of transfer admittance parameters in extracting a three-port transversal coupling matrix using MVF. The simulated responses of the extracted transversal coupling matrix that is corresponding to the fitting model obtained by MVF and the measured raw data of one of tuning states are superimposed in Fig. 5.

B. Helical Resonator Diplexer

Fig. 1(d) is the photograph of the helical resonator diplexer. The physical dimensions of the helical resonators are introduced in [15]. The wires connecting the first two resonators of the upper and lower band filters to the common port are with lengths of 24 and 21 mm, respectively. The lower and upper frequency bands of the diplexer are 690 MHz–803 GHz and 824–960 MHz, respectively. Thus $f_0 = 814$ MHz and $\text{BW} = 270$ MHz are used in frequency mapping (8).

Fig. 6 shows the coupling topology of the helical resonator diplexer with Δ -junction model. It can be told from the minimum path rule that there are six TZs in both S_{12} (Y_{12}) and S_{13} (Y_{13}), and two TZs in S_{23} (Y_{23}). To take possible parasitic couplings into consideration, the order of the numerators of Y_{12} , Y_{13} , and Y_{23} are fixed to be 7, 7, and 4, respectively.

For one tuning state of the helical resonator diplexer, the measured data and responses of the extracted transversal

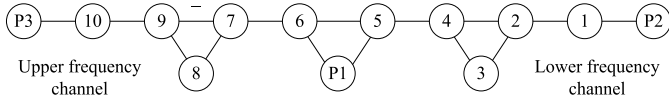


Fig. 6. Routing diagram of the helical resonator diplexer.

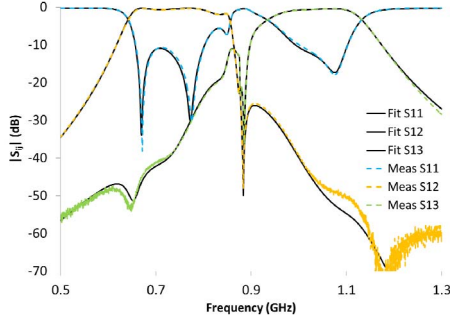


Fig. 7. Measured data and calculated responses of the extracted transversal coupling matrix of the helical resonator diplexer.

coupling matrix are plotted together in Fig. 7. Due to a relatively large fractional bandwidth (FBW $\approx 30\%$), small discrepancy can be observed when the rejection is below -50 dB.

IV. COUPLING MATRIX TRANSFORMATION

To establish one-to-one correspondence between the entries in the extracted coupling matrix and physical tuning elements, the diagnosed transversal coupling matrix from the extracted rational functions of admittance parameters must be transformed to the right form corresponding to the physical realization.

In a previous paper [11], a three-port coupling matrix transformation procedure is proposed for diplexers with resonant type of junction. In this section, a more general transformation strategy is introduced which is applicable to diplexers with tapped wire T -junction as well as common resonator junction. To illustrate the strategy clearly, the coupling topology of the combline diplexer will be discussed in detail.

A. General Transformation Strategy

The circuit model of a diplexer is described by a three-port coupling matrix

$$\mathbf{M} = \begin{bmatrix} \mathbf{M}_p & \mathbf{M}_{pn} \\ \mathbf{M}_{pn}^T & \mathbf{M}_n \end{bmatrix} \quad (9)$$

where \mathbf{M}_p is a 3-by-3 submatrix, \mathbf{M}_{pn} is a 3-by- n submatrix holding the I/O couplings, and \mathbf{M}_n is an n -by- n sub-matrix holding the self-couplings of the n resonators and the inter-resonator couplings. It has been shown that the responses of the three-port network do not change if \mathbf{M} is transformed by [16]

$$\mathbf{M}' = \mathbf{Q}^T \mathbf{M} \mathbf{Q} \quad (10)$$

where \mathbf{Q} is an orthogonal matrix represented by block submatrices as

$$\mathbf{Q} = \begin{bmatrix} \mathbf{I}_p & \mathbf{0}_{pn} \\ \mathbf{0}_{pn}^T & \mathbf{R}_n \end{bmatrix}. \quad (11)$$

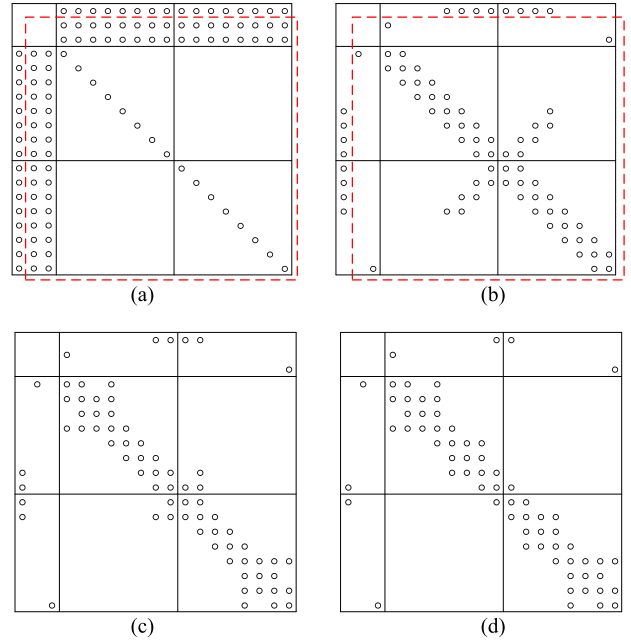


Fig. 8. Coupling matrix transformation procedure for the combline diplexer. (a) Transversal matrix. (b) Canonical form matrix. (c) Two quartets are split from the central cross couplings. (d) Final matrix corresponding to the coupling structure of Fig. 4. Hollow circles represent expected nonzero entries at each stage. The matrices are partitioned according to three ports, eight resonators in each channel filter.

In (11), \mathbf{I}_p is a 3-by-3 identity matrix and \mathbf{R}_n is an orthogonal matrix. Usually, \mathbf{R}_n is a rotation matrix which can be specified by the pivot $[i, j]$ and the rotation angle θ_r . Several coupling matrix reconfiguration strategies are available in [17] for obtaining a variety of coupling topologies of a bandpass filter. These strategies are also helpful in reconfiguration of a coupling matrix of a diplexer.

The main idea to transform the coupling matrix of a tapped wire T -junction diplexer is to treat the three-port network as a two-port network. If port 1 is the common port, ports 2 and 3 together with all the resonators can be reconfigured to “folded” form by the known transformation sequence. Throughout the matrix transformation procedure, the values of I/O couplings associated with the common port are subject to change, but no specific action needs to be taken to annihilate those couplings. After the coupling matrix is transformed to the desired form, the final values of the I/O couplings associated with the common port are automatically determined.

B. Illustrative Example

Following the general idea, the matrix transformation for the combline diplexer can be divided into three steps, as depicted in Fig. 8(a)–(d), where the rows and columns in the matrices are partitioned according to the three ports, the eight resonators in the lower band channel filter and the eight resonators in the upper band channel filter.

In the first step, the submatrix in the dashed line box in Fig. 8(a) and (b) is treated as a two-port filter (between ports 2 and 3) and is transformed to a “folded” form. The resultant matrix corresponds to a coupling diagram as depicted

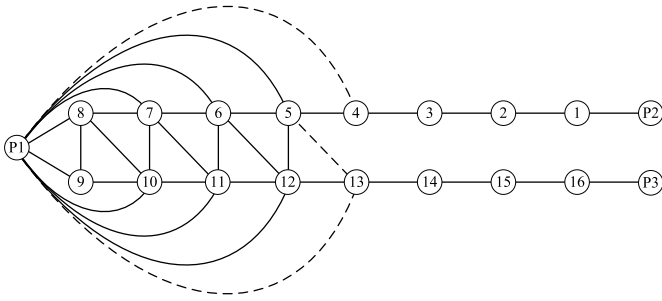


Fig. 9. Routing diagram corresponding to the coupling matrix reconfiguration stage in Fig. 8(b). Solid lines represent I/O couplings and interresonator couplings that exist in an ideal circuit which can be perfectly transformed to the one in Fig. 4. Dashed lines represent stray couplings.

in Fig. 9, in which P1 is cross-coupled to several resonators in both channel filters. P1, P2, and resonators number 1 through 8 are in an “arrow” form [18], where the number of nonzero cross-couplings is determined by the number of TZs in S_{12} . So are P1, P3, and resonators number 9 through 16. P1, P2, and all the 16 resonators are in a “folded” form, where the number of nonzero cross-couplings is determined by the number of TZs of S_{23} . This topology is a canonical form for duplexers since it can be uniquely determined by a prescribed sequence of similarity transformations [19].

In the second step, the two quartets are split with the method proposed in [20]. After the two quartets are pulled to the right places, the remaining coupling matrix is expected to be in the form of Fig. 8(c). In the final step, the two tri-sections are split by the same method, and the coupling matrix of the desired form corresponding to Fig. 4 can be obtained.

In the last two steps, the rotation angle θ_r of the orthogonal matrix \mathbf{Q} in (11) is determined by the locations of corresponding TZs. Therefore, identification of the TZs is necessary to obtain a cascaded coupling topology.

V. IMPLEMENTATION IN PRACTICE

Note that the procedure discussed in previous section is for ideal circuits, which can be perfectly transformed to the desired form. However, in a practical CAT problem there will be many stray couplings, as will be seen in this section.

A. Identification and Association of TZs

In the combline diplexer, both channel filters have the form of a tri-section cascaded with a quartet. Theoretically, a tri-section can introduce a single TZ on the imaginary axis, and a quartet can create either two TZs on the imaginary axis or a pair of complex TZs symmetrically located about the imaginary axis on the s -plane.

The diagnosed transversal coupling matrix is first transformed to the canonical form of Fig. 9. In practice, cross couplings with absolute values smaller than 10^{-4} can be discarded at this stage. Nevertheless, it is found that the extracted coupling matrix still has three additional cross-couplings as compared to those of an ideal case, which are $M_{P1,4}$, $M_{P1,13}$, and $M_{5,13}$, as shown in Fig. 9 with dashed lines.

In order to proceed with the coupling matrix reconfiguration procedure, the locations of TZs need to be known. Once the

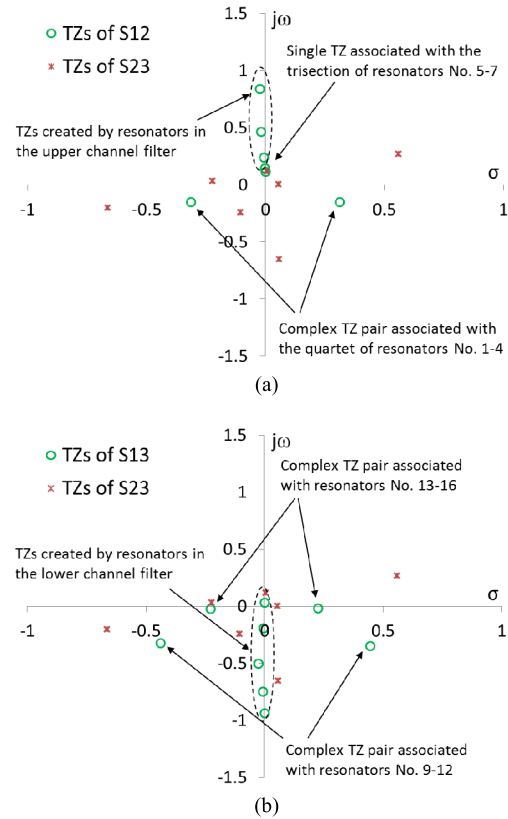


Fig. 10. TZs of the combline diplexer from one tuning state. (a) Distribution of the TZs of S_{12} and S_{23} . (b) Distribution of the TZs of S_{13} and S_{23} .

extracted transversal coupling matrix is transformed to the canonical form, the submatrix containing resonators number 4–13 is taken out and the subnetwork is analyzed. One can obtain the close-form characteristic functions as a reversing procedure of synthesis. By computing the zeros of the transfer functions, the locations of the TZs can be obtained. For one tuning state, the TZ distribution of the subnetwork is plotted in Fig. 10(a) and (b).

Theoretically, a TZ of S_{23} is also a TZ of either S_{12} or S_{13} , because TZs of S_{23} are created by the tri-sections/quartets which are shared with the path from Ports 1 to 2/3. These TZs either locate on the imaginary axis or come in symmetric pairs about the imaginary axis. In addition, S_{12} and S_{13} have several complex TZs on the left-half s -plane which are created by the resonators from the other channel filter. However, in practice most of diagnosed TZs of S_{23} do not coincide with any TZ of S_{12} and S_{13} , as can be seen in Fig. 10(a) and (b). Since measured S_{23} data are very small in magnitude over the entire frequency range, the diagnosed TZs of S_{23} cannot be very accurate. Therefore, suitable TZs of S_{12} and S_{13} are adopted and assigned to the tri-section/quartet in the coupling matrix reconfiguration procedure.

The complex TZ pair of S_{12} associated with the quartet composed of resonators number 1 through 4 can be clearly seen in Fig. 10(a). The single TZ associated with the tri-section of resonators number 5 through 7 can also be easily identified since this TZ is shared by S_{12} and S_{23} and it locates on the imaginary axis.

TABLE I
EXTRACTED COUPLING MATRIX OF THE COMBLINE DIPLEXER

	P1	P2	P3	1	2	3	4	5	6	7	8	9	10	11	12	13	14	15	16
P1	0.0016 -0.0029i	0	0	0	0	0	0	0	0.0005 +0.0002i	0.0229 +0.0008i	0.5174 +0.0047i	0.8756 -0.0067i	0.0065 +0.0007i	0.0020 -0.0001i	0	0	0	0	0
P2	0	0.0008 -0.0077i	0	0.6916 -0.0024i	0	0	0	0	0	0	0	0	0	0	0	0	0	0	0
P3	0	0	0.0004 -0.0078i	0	0	0	0	0	0	0	0	0	0	0	0	0	0	0	0.7662 -0.0026i
1	0	0.6916 -0.0024i	0	0.6475 -0.0052i	0.3562 -0.0001i	0	0.0878 -0.0003i	0	0	0	0	0	0	0	0	0	0	0	0
2	0	0	0	0.3562 -0.0001i	0.6094 -0.0016i	0.2426 +0.0001i	0.1586 -0.0002i	0	0	0	0	0	0	0	0	0	0	0	0
3	0	0	0	0	0.2426 +0.0001i	0.3381 -0.0021i	0.1951 -0.0001i	0	0	0	0	0	0	0	0	0	0	0	0
4	0	0	0	0.0878 -0.0003i	0.1586 -0.0002i	0.1951 -0.0001i	0.5753 -0.0018i	0.2559 -0.0001i	0	0	0	0	0	0	0.0001	-0.0001	0	0	0
5	0	0	0	0	0	0	0.2559 -0.0001i	0.5632 -0.0018i	0.2173	0.0881	0	0	0	0	0.0001	0	0	0	0
6	0.0005 +0.0002i	0	0	0	0	0	0	0.2173	0.5160 -0.0020i	0.2564 -0.0001i	0	0	0	0	0.0005	0	0	0	0
7	0.0229 +0.0008i	0	0	0	0	0	0	0.0881	0.2564 -0.0001i	0.2902 -0.0014i	0.3884	0.0131 -0.0016i	0.0025 -0.0019i	0.0013 +0.0005i	0.0003 -0.0004i	0	0	0	0
8	0.5174 +0.0047i	0	0	0	0	0	0	0	0.3884	0.8502 -0.0034i	0.3524 -0.0148i	0	0	0	0	0	0	0	0
9	0.8756 -0.0067i	0	0	0	0	0	0	0	0.0131 -0.0016i	0.3524 -0.0148i	0.8026 -0.0178i	0.4072 -0.0012i	0	0.0267	0	0	0	0	0
10	0.0065 +0.0007i	0	0	0	0	0	0	0	0	0.4072 -0.0012i	-0.6071 -0.0013i	0.2311 -0.0005i	-0.1104 -0.0009i	0	0	0	0	0	0
11	0.0020 -0.0001i	0	0	0	0	0	0	0	0	0	0	0.2311 -0.0005i	-0.4136 +0.0001i	0.2282 -0.0004i	0	0	0	0	0
12	0	0	0	0	0	0	0.0001	0.0001	0.0005	0.0003 -0.0004i	0	0.0267	-0.1104 -0.0009i	0.2282 -0.0004i	-0.5975 +0.0018i	0.2263 +0.0001i	0	0	0
13	0	0	0	0	0	0	-0.0001	0	0	0	0	0	0	0	0.2263 +0.0001i	-0.5531 -0.0017i	0.1871 +0.0002i	-0.1726 +0.0009i	0.0698 -0.0004i
14	0	0	0	0	0	0	0	0	0	0	0	0	0	0	0	0.1871 +0.0002i	-0.3099 -0.0025i	0.1816 +0.0004i	0
15	0	0	0	0	0	0	0	0	0	0	0	0	0	0	0	-0.1726 +0.0009i	0.1816 +0.0004i	-0.6300 -0.0025i	0.3951 -0.0001i
16	0	0	0.7662 -0.0026i	0	0	0	0	0	0	0	0	0	0	0	0	0.0698 -0.0004i	0	0.3951 -0.0001i	-0.6151 -0.00062i

TABLE II
EXTRACTED COUPLING MATRIX OF THE HELICAL RESONATOR DIPLEXER

	P1	P2	P3	1	2	3	4	5	6	7	8	9	10
P1	0.0325 -0.0203i	0	0	0	0	0	0.0675 -0.0027i	0.5872 -0.0061i	0.9931 +0.0036i	-0.0125 +0.0018i	0.0033 +0.0002i	0	0
P2	0	-0.0039 -0.0128i	0	0.7666 +0.0019i	0	0	0	0	0	0	0	0	0
P3	0	0	0.0155 -0.0031i	0	0	0	0	0	0	0	0	0	0.7984 +0.0002i
1	0	0.7666 +0.0019i	0	0.5835 -0.0081i	0.3643 +0.0001i	0	0	0	0	0	0	0	0
2	0	0	0	0.3643 +0.0001i	0.5851 -0.002i	0.2270 -0.0001i	0.1957 +0.0005i	0	0	0	0	0	0
3	0	0	0	0	0.2270 -0.0001i	0.2405 -0.0033i	0.2194 -0.0001i	0	0	0	0	0	0
4	0.0675 -0.0027i	0	0	0	0.1957 +0.0005i	0.2194 -0.0001i	0.5875 -0.0037i	0.4196 -0.0008i	0.0536 -0.0013i	0	-0.0035 -0.0002i	0	0
5	0.5872 -0.0061i	0	0	0	0	0	0.4196 -0.0008i	0.7037 -0.0056i	0.4398 +0.0002i	0	0	0	0
6	0.9931 +0.0036i	0	0	0	0	0	0.0536 -0.0013i	0.4398 +0.0002i	-0.3934 -0.0118i	0.4296 -0.0001i	0	0	0
7	-0.0125 +0.0018i	0	0	0	0	0	0	0	0.4296 -0.0001i	-0.3403 -0.0015i	0.2090 +0.0005i	-0.2380 -0.0005i	0
8	0.0033 +0.0002i	0	0	0	0	0	-0.0035 -0.0002i	0	0	0.2090 +0.0005i	-0.2093 -0.0021i	0.2138 -0.0006i	0
9	0	0	0	0	0	0	0	0	0	-0.2380 -0.0005i	0.2138 -0.0006i	-0.4547 -0.0034i	0.4068 +0.0003i
10	0	0	0.7984 +0.0002i	0	0	0	0	0	0	0	0	0.4068 +0.0003i	-0.6024 -0.0074i

The TZs of the upper frequency channel filter are plotted in the complex plane as shown in Fig. 10(b). Two complex TZ pairs of S_{13} are observed which is not expected since there is only one quartet in the channel filter. One of the TZ pairs is believed to be the result of parasitic coupling between resonators number 9 and 12 due to the dumbbell-shape probe and another quartet is formed.

In the tuning process, one needs to identify the association of the two TZ pairs with the two quartets in physical realization. By a simple perturbation on related tuning screws, it can be identified that the upper TZ pair in the complex

plane is associated with the quartet composed of resonators number 13 through 16 and the lower pair is associated with the quartet of resonators number 9 through 12.

With subsequent matrix transformations, the final coupling matrix with real parts of all mainline couplings positive is given in Table I.

B. Stray Couplings and Unloaded Qs

The extracted transversal coupling matrix of the helical resonator diplexer is also first transformed to its canonical form, which is depicted in Fig. 11. There are many stray

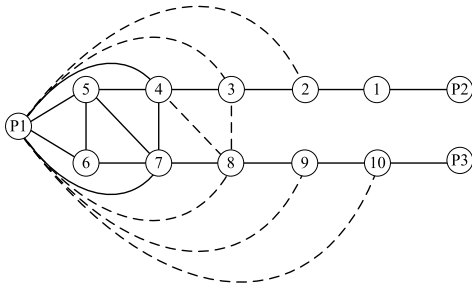


Fig. 11. Canonical form of the topology of the helical resonator diplexer. Solid lines represent couplings that exist in an ideal circuit. Dashed lines are stray couplings existed in an extracted coupling matrix of the diplexer.

couplings as a result of the relatively large FBW, which are shown with dashed lines. By a similar TZ identification procedure and subsequent transformations, the finally obtained coupling matrix is given in Table II.

Since the similarity transformation procedure does not change the responses of the network, the responses given by the final coupling matrices in Tables I and II are the same with those given by the transversal matrix as plotted in Figs. 5 and 7, respectively, except for some small round-off errors.

The final coupling matrices are obtained by applying similarity transformations to the extracted transversal coupling matrix. Although the best effort is made to convert the matrix to a form that matches the topology of the physical realization, the results can still contain a lot of stray couplings that cannot be mapped to any physical coupling element, which are shown in red color in Tables I and II. These nonphysical stray couplings are attributed to parasitic couplings, spurious resonance, dispersive effects and possibly other nonideal effects in measurement or fitting procedure. Although the absolute values of stray couplings are very small as compared to intentionally designed couplings, they have significant influence on the responses of the extracted coupling matrix and cannot be ignored in the fine tuning stage of the diplexer. Therefore, an adaptive CAT strategy will be proposed in the next section.

It can be seen that extracted coupling matrices have imaginary parts, and the unloaded Q of the i th resonator is related to the imaginary part of corresponding diagonal entry by

$$Q_i = -\frac{f_0}{\text{BW}} \frac{1}{\text{Im}\{M_{ii}\}}. \quad (12)$$

With (12) the unloaded Q of resonators can be well-estimated for low Q devices. However, for high Q resonators, the imaginary part of corresponding self-coupling term is too small that the accuracy of the obtained Q value is not guaranteed.

In the adaptive CAT to be introduced in the next section, the values of Q do not directly take part in the optimization. The imaginary parts of the coupling matrix are fixed during the optimization process.

VI. ADAPTIVE COMPUTER-AIDED TUNING

It can be seen from the extracted matrices in Tables I and II that they contain two kinds of nonideal components: 1) stray couplings which are not possible to be fully considered in

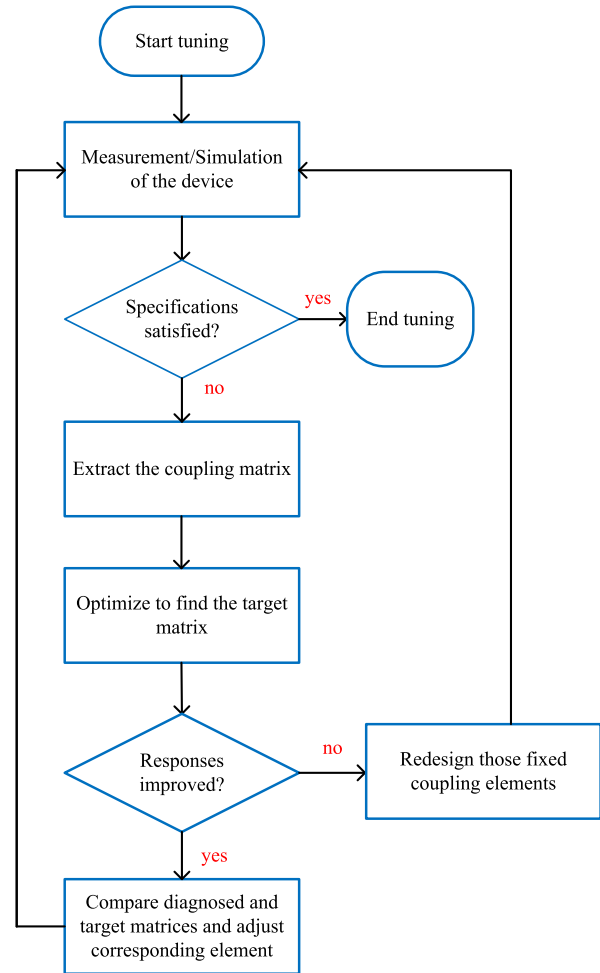


Fig. 12. Flowchart of the adaptive CAT procedure.

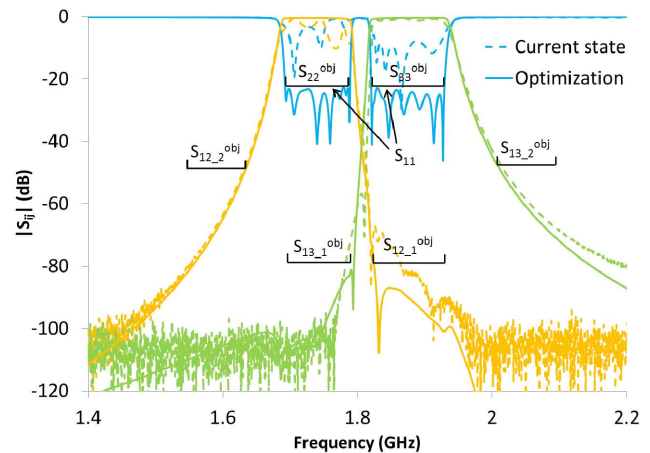


Fig. 13. Illustration of the adaptive CAT procedure. Dashed lines: currently measured responses. Solid lines: responses of the optimized coupling matrix in Table III.

the initial design and 2) the imaginary parts of the extracted coupling matrix that count for power dissipation. In addition, some of the coupling elements cannot be easily or continuously tuned, such as the T -junction, the capacitive probe in the combline diplexer and tapped line for realizing inductive couplings in the helical resonator diplexer. Considering all these facts, the coupling matrix used in initial design is not suitable to serve as a constant tuning target.

TABLE III
OPTIMIZED TARGET COUPLING MATRIX BASED ON THE EXTRACTED COUPLING MATRIX IN TABLE I

	P1	P2	P3	1	2	3	4	5	6	7	8	9	10	11	12	13	14	15	16	
P1	0.0016 -0.0029i	0	0	0	0	0	0	0	0.0005 +0.0002i	0.0229 +0.0008i	0.5174 +0.0047i	0.8756 -0.0067i	0.0065 +0.0007i	0.0020 -0.0001i	0	0	0	0	0	
P2	0	0.0008 -0.0077i	0	0.6916 -0.0024i	0	0	0	0	0	0	0	0	0	0	0	0	0	0	0	
P3	0	0	0.0004 -0.0078i	0	0	0	0	0	0	0	0	0	0	0	0	0	0	0	0.7662 -0.0026i	
1	0	0.6916 -0.0024i	0	0.5564 -0.0052i	0.3703 -0.0001i	0	0.0878 -0.0003i	0	0	0	0	0	0	0	0	0	0	0	0	
2	0	0	0	0.3703 -0.0001i	0.4992 -0.0016i	0.1596 +0.0001i	0.1586 -0.0002i	0	0	0	0	0	0	0	0	0	0	0	0	
3	0	0	0	0	0.1596 +0.0001i	0.2741 -0.0021i	0.1816 -0.0001i	0	0	0	0	0	0	0	0	0	0	0	0	
4	0	0	0	0.0878 -0.0003i	0.1586 -0.0002i	0.1816 -0.0001i	0.6025 -0.0018i	0.2373 -0.0001i	0	0	0	0	0	0	0.0001	-0.0001	0	0	0	
5	0	0	0	0	0	0	0.2373 -0.0001i	0.5943 -0.0018i	0.2257	0.0881	0	0	0	0	0.0001	0	0	0	0	
6	0.0005 +0.0002i	0	0	0	0	0	0	0.2257	0.4189 -0.0020i	0.2454 -0.0001i	0	0	0	0	0.0005	0	0	0	0	
7	0.0229 +0.0008i	0	0	0	0	0	0.0881	0.2454 -0.0001i	0.5958 -0.0014i	0.3510	0.0131 -0.0016i	0.0025 -0.0019i	0.0013 +0.0005i	0.0003 -0.0004i	0	0	0	0	0	
8	0.5174 +0.0047i	0	0	0	0	0	0	0	0.3510	0.7651 -0.0034i	0.3524 -0.0148i	0	0	0	0	0	0	0	0	
9	0.8756 -0.0067i	0	0	0	0	0	0	0	0	0.0131 -0.0016i	0.3524 -0.0148i	0.6297 -0.0178i	0.3897 -0.0012i	0	0.0267	0	0	0	0	
10	0.0065 +0.0007i	0	0	0	0	0	0	0	0	0.0025 -0.0019i	0	0.3897 -0.0012i	0.2264 -0.0005i	-0.1104 -0.0009i	0	0	0	0	0	
11	0.0020 -0.0001i	0	0	0	0	0	0	0	0	0.0013 +0.0005i	0	0	0.2264 -0.0005i	-0.3745 +0.0001i	0.2286 -0.0004i	0	0	0	0	
12	0	0	0	0	0	0	0.0001	0.0001	0.0005	0.0003 -0.0004i	0	0.0267	-0.1104 -0.0009i	0.2286 -0.0004i	-0.5926 -0.0001i	0.2496 +0.0001i	0	0	0	
13	0	0	0	0	0	0	-0.0001	0	0	0	0	0	0	0	0.2496 +0.0001i	-0.5998 -0.0017i	0.1901 +0.0002i	-0.1726 +0.0009i	0.0698 -0.0004i	
14	0	0	0	0	0	0	0	0	0	0	0	0	0	0	0	0.1901 +0.0002i	-0.2454 -0.0025i	0.1857 +0.0004i	0	
15	0	0	0	0	0	0	0	0	0	0	0	0	0	0	0	0	-0.1726 +0.0009i	0.1857 +0.0004i	-0.4971 -0.0025i	0.4248 -0.0001i
16	0	0	0.7662 -0.0026i	0	0	0	0	0	0	0	0	0	0	0	0	0.0698 -0.0004i	0	0.4248 -0.0001i	-0.5392 -0.0062i	

After the coupling matrix is extracted from the measured responses, only those entries corresponding to tuning screws are picked out, and their real parts are chosen as the variables in an optimization for the target coupling matrix. The extracted coupling values are used as the initial values, and a proper lower and upper bound can be set considering the realistic tuning range of each tuning element. The stray couplings, the couplings that are not easily or continuously adjustable, and the imaginary parts of the matrix are fixed in the optimization process. A proper cost function is set according to the design specifications.

At the preliminary tuning stage, it is not necessary to push the optimization process to the limit of the cost function as long as the optimized coupling matrix can give improved responses over those of the current tuning state. At the fine tuning stage extracted coupling values can offer a good set of initial values for the optimization such that it can be finished in a few iterations.

By comparing the optimized target matrix with the extracted one, one can easily identify which tuning screws need to be adjusted. Although adjustment of the tuning screw mainly changes the real part of corresponding entry in the matrix, stray couplings as well as the imaginary parts of the coupling matrix will also be affected. Rather than uniformly using one target coupling matrix from beginning to end, the adaptive CAT strategy continuously updates the target coupling matrix based on newly extracted coupling matrix. The tuning-and-optimization process is repeated until either the response meets the design specifications or optimization on chosen variables cannot improve the responses any more. Usually in the latter

case, some fixed couplings, such as the tapped wire T -junction or cross coupling elements, need to be adjusted or redesigned. The whole adaptive CAT procedure is summarized in Fig. 12.

In the adaptive tuning process of the combline diplexer, only real parts of self-couplings and mainline couplings (excluding M_{89}) are chosen as the optimization variables, which are shown in bold black fonts in Table I. The objective is to achieve 22 dB return loss (RL), 80 dB isolation between the two channels and 50 dB out of band rejection. A MiniMax objective function is set to

$$K = |S_{11}| + |S_{22}| + |S_{33}| + (|S_{12_1}| + |S_{13_1}| + |S_{12_2}| + |S_{13_2}|)/4 \quad (13)$$

where $|S_{11}|$, $|S_{22}|$, and $|S_{33}|$ denote the maximum RL at ports 1–3, respectively, within the corresponding passbands. $|S_{12_1}|$ and $|S_{13_1}|$ denote the poorest rejection level between the two channels. $|S_{12_2}|$ and $|S_{13_2}|$ denote the poorest rejection on the outer sides of the channel filters. All the variables in (13) are in decibel (dB) and the specs are marked in Fig. 13. In the optimization process when a term in (13) is below the target value the term will be set to the same value as the target.

The optimized target matrix based on the extracted coupling matrix in Table I is shown in Table III, whose responses are plotted with solid lines in Fig. 13. By comparing the real parts of the entries in Tables I and III, one can find out the entries with large differences, such as M_{77} in this case, and then go to adjust the corresponding physical tuning elements. Fig. 14(a)–(d) shows four tuning states of the combline

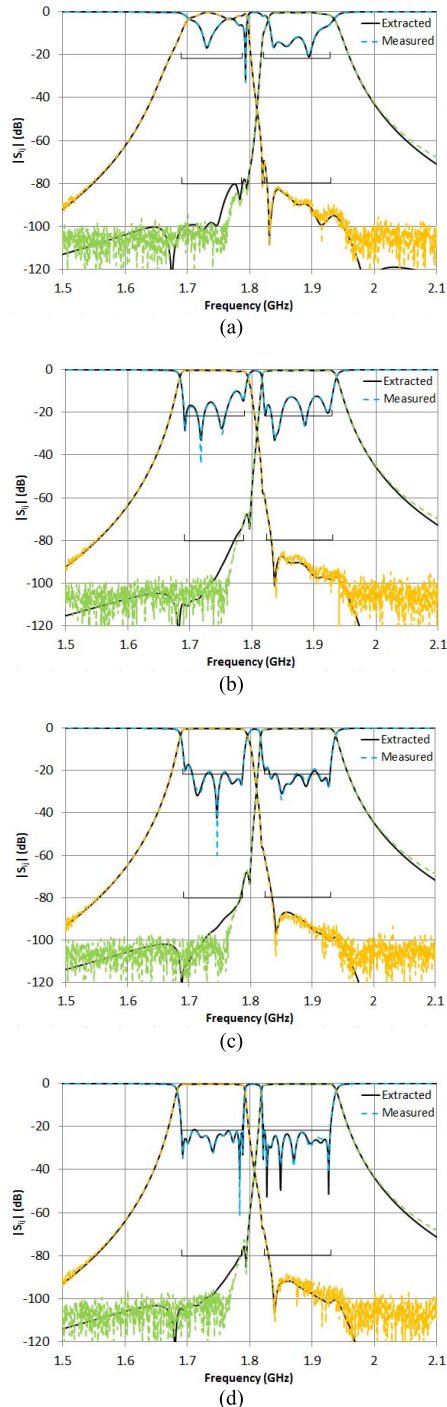


Fig. 14. Four tuning states of the test diplexer in the adaptive CAT process. Solid lines are responses given by the extracted coupling matrix. Dashed lines are measured data.

diplexer together with the responses given by the extracted coupling matrices.

VII. CONCLUSION

With the theory for tapped wire T -junction established in this paper, it is demonstrated that MVF can be applied to a coupled-resonator diplexer with a tapped wire T -junction for extracting its circuit model. A more general coupling matrix transformation scheme for the diplexers is introduced

to reconfigure the transversal matrix to the one corresponding to the physical realization.

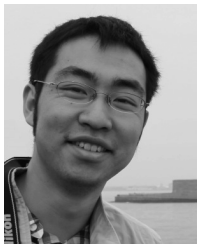
As demonstrated by two examples, in the extracted coupling matrix there are many stray couplings that cannot be annihilated or discarded, and they do not correspond to physical tuning elements. To deal with those stray couplings, an adaptive CAT strategy is proposed, which takes those stray couplings into account in its dynamically optimized target coupling matrix based on the previous tuning state. The adaptive CAT has been proven to be an effective dynamic decision-making process.

The most challenging part in the CAT procedure is identifying the TZs associated with each tri-section/quartet, because it can involve a multiple-solution problem. To apply the CAT technique proposed in this paper to a general class of diplexers and other coupled-resonator devices, a systematic and reliable method is needed to identify the true association of TZs with each tri-section/quartet.

REFERENCES

- [1] J. B. Ness, "A unified approach to the design, measurement, and tuning of coupled-resonator filters," *IEEE Trans. Microw. Theory Techn.*, vol. 46, no. 4, pp. 343–351, Apr. 1998.
- [2] M. Kahrizi, S. Safavi-Naeini, S. Chaudhuri, and R. Sabry, "Computer diagnosis and tuning of RF and microwave filters using model-based parameter estimation," *IEEE Trans. Circuits Syst. I, Fundam. Theory Appl.*, vol. 49, no. 9, pp. 1263–1270, Sep. 2002.
- [3] G. Pepe, F. J. Gortz, and H. Chaloupka, "Sequential tuning of microwave filters using adaptive models and parameter extraction," *IEEE Trans. Microw. Theory Techn.*, vol. 53, no. 1, pp. 22–31, Jan. 2005.
- [4] M. Meng and K.-L. Wu, "An analytical approach to computer-aided diagnosis and tuning of lossy microwave coupled resonator filters," *IEEE Trans. Microw. Theory Techn.*, vol. 57, no. 12, pp. 3188–3195, Dec. 2009.
- [5] A. G. Lamperez, T. K. Sarkar, and M. S. Palma, "Generation of accurate rational models of lossy systems using the Cauchy method," *IEEE Microw. Wireless Compon. Lett.*, vol. 14, no. 10, pp. 490–492, Oct. 2004.
- [6] G. Macchiarella, "Extraction of unloaded Q and coupling matrix from measurements on filters with large losses," *IEEE Microw. Wireless Compon. Lett.*, vol. 20, no. 6, pp. 307–309, Jun. 2010.
- [7] P. Zhao and K.-L. Wu, "A new computer-aided tuning scheme for general lossy coupled-resonator bandpass filters based on the Cauchy method," *HKIE Trans.*, vol. 23, no. 1, pp. 52–62, Mar. 2016.
- [8] H. Hu and K.-L. Wu, "A generalized coupling matrix extraction technique for bandpass filters with uneven- Q s," *IEEE Trans. Microw. Theory Techn.*, vol. 62, no. 2, pp. 244–251, Feb. 2014.
- [9] D. Traina, G. Macchiarella, and T. K. Sarkar, "Robust formulations of the cauchy method suitable for microwave diplexers modeling," *IEEE Trans. Microw. Theory Techn.*, vol. 55, no. 5, pp. 974–982, May 2007.
- [10] M. Oldoni, F. Seyfert, G. Macchiarella, and D. Pacaud, "Deembedding of filters' responses from diplexer measurements," in *IEEE MTT-S Int. Microw. Symp. Dig.*, Jun. 2011, pp. 1–4.
- [11] P. Zhao and K.-L. Wu, "Model-based vector-fitting method for circuit model extraction of coupled-resonator diplexers," *IEEE Trans. Microw. Theory Techn.*, vol. 64, no. 6, pp. 1787–1797, Jun. 2016.
- [12] G. Macchiarella, M. Oldoni, and S. Tamiasso, "Narrowband microwave filters with mixed topology," *IEEE Trans. Microw. Theory Techn.*, vol. 60, no. 12, pp. 3980–3987, Dec. 2012.
- [13] P. Zhao and K.-L. Wu, "An iterative and analytical approach to optimal synthesis of a multiplexer with a star-junction," *IEEE Trans. Microw. Theory Techn.*, vol. 62, no. 12, pp. 3362–3369, Dec. 2014.
- [14] R. J. Cameron, C. M. Kudsia, and R. R. Mansour, *Microwave Filters for Communication Systems: Fundamentals, Design and Applications*, Hoboken, NJ, USA: Wiley, 2007, p. 222.
- [15] P. Zhao, Z. Li, J. Wu, K.-L. Wu, and Y. Cui, "A compact wideband UHF helical resonator diplexer," in *IEEE MTT-S Int. Microw. Symp. Dig.*, San Francisco, CA, USA, May 2016, pp. 1–3.

- [16] A. Garcia-Lamperez and M. Salazar-Palma, "Analytical synthesis of coupling matrices for N-port networks with reactance compensation," presented at the Eur. Microw. Week Workshop Adv. N-port Netw. Space Appl., Amsterdam, The Netherlands, Oct. 2012.
- [17] R. J. Cameron, C. M. Kudsia, and R. R. Mansour, *Microwave Filters for Communication Systems: Fundamentals, Design and Applications*, Hoboken, NJ, USA: Wiley, 2007, ch. 8–10.
- [18] H. C. Bell, Jr., "Canonical asymmetric coupled-resonator filters," *IEEE Trans. Microw. Theory Techn.*, vol. MTT-30, no. 9, pp. 1335–1340, Sep. 1982.
- [19] G. Macchiarella and S. Tamiazzo, "Generation of canonical forms for multiport filtering networks," in *IEEE MTT-S Int. Microw. Symp. Dig.*, Tampa, FL, USA, Jun. 2014, pp. 1–3.
- [20] S. Tamiazzo and G. Macchiarella, "An analytical technique for the synthesis of cascaded N-tuplets cross-coupled resonators microwave filters using matrix rotations," *IEEE Trans. Microw. Theory Techn.*, vol. 53, no. 5, pp. 1693–1698, May 2005.



Ping Zhao (S'14) received the B.Sc. degree from Nanjing University, Nanjing, China, in 2012. He is currently pursuing the Ph.D. degree at The Chinese University of Hong Kong, Hong Kong.

His current research interests include synthesis and computer-aided tuning algorithms for multiport microwave coupled-resonator networks, including diplexers, multiplexers and coupled-resonator decoupling networks with applications in cellular base stations, and satellites.

Mr. Zhao was a recipient of the Honorable Mention in the 2014 International Microwave Symposium Student Paper Competition. He was a recipient of the Best Student Paper Award of the 2014 IEEE HK AP/MTT Postgraduate Conference.



Ke-Li Wu (M'90–SM'96–F'11) received the B.S. and M.Eng. degrees from the Nanjing University of Science and Technology, Nanjing, China, in 1982 and 1985, respectively, and the Ph.D. degree from Laval University, Quebec, QC, Canada, in 1989.

From 1989 to 1993, he was a Research Engineer with the Communications Research Laboratory, McMaster University, Hamilton, ON, Canada, where he was also a Group Manager. In 1993, he joined the Corporate Research and Development Division, COM DEV International, Cambridge, ON, where he

was a Principal Member of Technical Staff. Since 1999, he has been with The Chinese University of Hong Kong, Hong Kong, where he is a Professor and the Director of the Radio frequency Radiation Research Laboratory. He has authored numerous publications in the areas of EM modeling and microwave passive components, microwave filter and antenna engineering. His current research interests include partial element equivalent circuits and physically derived micromodeling circuits for high-speed circuits, RF and microwave passive circuits and systems, synthesis theory and robot automatic tuning of microwave filters, decoupling techniques for multiple antennas in both wireless terminals, and massive multi-in multi-out array antennas.

Prof. Wu is a member of the IEEE Microwave Theory and Technique (MTT)-8 subcommittee (Filters and Passive Components) and also serves as a TPC member for many prestigious international conferences including the IEEE MTT-S International Microwave Symposium. He was a recipient of the 1998 COM DEV Achievement Award for the development of exact EM design software of microwave filters and multiplexers and the Asia-Pacific Microwave Conference Prize in 2008 and 2012, respectively. From 2006 to 2009, he was an Associate Editor of the IEEE TRANSACTIONS ON MICROWAVE THEORY AND TECHNIQUES.